

PHOTO PRODUCTION OF ISOTOPES FOR MEDICAL AND INDUSTRIAL USAGES

Barbara Szpunar and Chary Rangacharyulu
Department of Physics and Engineering Physics,
University of Saskatchewan, Saskatoon, SK S7N 5E2

Abstract

Photo-neutron reactions induced by ~15 MeV photons offer an attractive option to produce the isotopes of interest for medical and industrial applications. In this article, we present the results of simulations using FLUKA Monte Carlo code on the $^{100}\text{Mo}(\gamma,n)^{99}\text{Mo}$ and $^{193}\text{Ir}(\gamma,n)^{192}\text{Ir}$ processes of great interest to medical industry. It is seen that the ^{99}Mo decaying to $^{99\text{m}}\text{Tc}$ and the ^{192}Ir are copiously produced. In contrast to the conventional bremsstrahlung photon beam sources, the laser back scatter photon sources at electron synchrotrons provide the selective tuning capability of photons of energies of interest. This feature coupled with the ubiquitous Giant Dipole Resonance excitations of atomic nuclei promise a fertile ground of nuclear isotope productions. It is suggested that a new photon beam-line at the Canadian Light Source can serve as a test ground for this purpose.

1. Introduction

In recent years, there has been a lot of interest and discussions among the Health Industry, the Governments and the Public for the supply of medical isotopes. The most commonly talked about issue was the shortage of supply as the Canada's NRU reactor is side-lined and the MAPLE reactors are in a holding pattern for technical reasons. This led to several proposals of new nuclear reactors and accelerator based isotope production facilities [1,2,3].

It is to be noted that *the University of Saskatchewan proposal [1] calls for a multipurpose reactor* which can take a few years before it is built and commissioned. *The proposal of groups from Sherbrooke and other organizations [2] seeks to employ proton beams from a cyclotron facility.* They propose to make use of $^{100}\text{Mo}(p,2n)$ reaction to produce $^{99\text{m}}\text{Tc}$ of a short half-life $T_{1/2} = 6.0$ hours. *The Prairie Isotope Production Enterprise (PIPE) [3] calls for a photon induced reaction $^{100}\text{Mo}(\gamma,n)^{99}\text{Mo}$ using bremsstrahlung radiation from an electron linear accelerator.* As the proponents themselves realized, the downside of Sherbrooke proposal is that it yields the short-lived isotope limiting its use to supply for areas in the vicinity of the production center. The PIPE proposal employs bremsstrahlung beams and one has to contend with excessive background radiations and the by-products.

We suggest that the modern photon beam facilities such as the laser back scatter systems at the electron synchrotron sources used in conjunction with salient nuclear excitations have a good potential to produce medical isotopes in a more cost effective way with

minimal background radiations. This article describes the physics principle, and preliminary Monte Carlo simulations for the production of ^{99}Mo and ^{192}Ir isotopes, which find extensive applications in medicine. Also, basic laser back scatter parameters in context with the Canadian Light Source (CLS) facility are described.

2. Nuclear transmutation

As we consider the nuclear transmutation, it is helpful to examine the features of excitation spectrum of an atomic nucleus. A typical nucleus exhibits a few discrete levels, which de-excite by photon emission (Figure 1). The average binding energy per nucleon is about 8 MeV for intermediate mass nuclei ($A \sim 50-100$) and ~ 7 MeV for heavy nuclei ($A > 150$). This decrease in binding energy of heavy nuclei in comparison to that of intermediate mass nuclei is the source of nuclear energy as heavy ones undergo nuclear fission from less stable and more energetic systems to more stable and less energetic configurations.

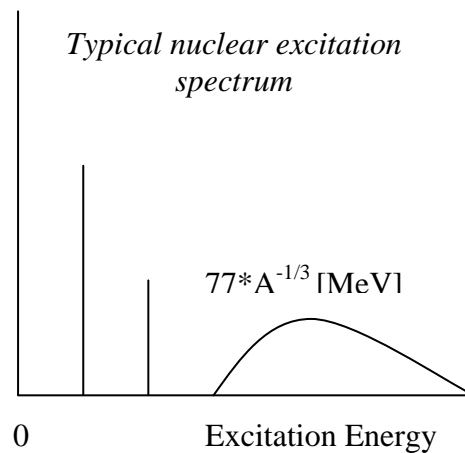


Figure 1. Typical nuclear excitation spectrum.

Above the particle threshold, all nuclei exhibit an isovector giant dipole resonance (GDR), easily excited by several probes, including photons. First discovered in 1947, the giant resonances have been extensively studied across the periodic table. From the systematics, it is well established that the centroid of these resonances are at an excitation energy of $E \text{ (MeV)} \approx 77 * A^{-1/3}$ and of decay widths $\Gamma \text{ (MeV)} \approx 23 * A^{-1/3}$ [4].

The Figure 2 shows plots of the GDR centroid (solid line) and width (dashed line) versus the mass number. For medium weight and heavy nuclei, the centroid is at 20-15 MeV. The lower curve is the width of the resonance which is about 5-3 MeV. A note-worthy feature is the monotonous decrease of the excitation energy to about 14 MeV for the mass number $A \sim 200$ and the width of about 4 MeV, which renders them excitable with photons of just above 10 MeV.

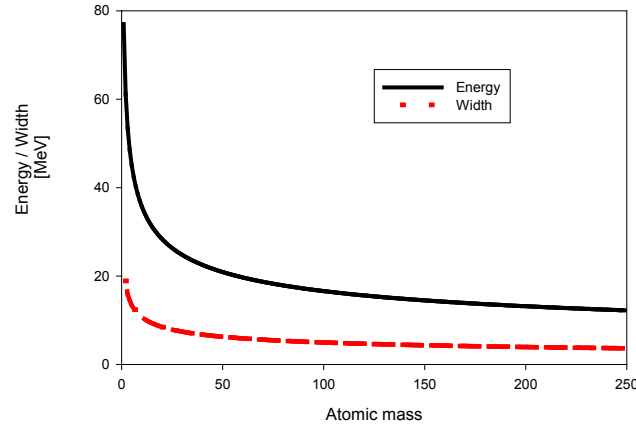


Figure 2. The Giant Dipole Resonance centroid (solid line) and the width (dashed line) versus the mass number.

A glance at the nuclear data tables will convince one that several medical isotopes can be produced using photon-nuclear reactions at tagged photon energy via the GDR decay by emitting neutrons. In Figure 3, the latest, available on <http://www.nndc.bnl.gov> [5,6], cross sections for (p,2n) reaction ($^{100}\text{Mo} \rightarrow ^{99\text{m}}\text{Tc}$), are compared with cross section for photo-nuclear (γ, n) reactions for ^{99}Mo ($^{100}\text{Mo} \rightarrow ^{99}\text{Mo}$) [7] and ^{192}Ir ($^{193}\text{Ir} \rightarrow ^{192}\text{Ir}$) [8]. Some earlier data for the cross sections of $^{100}\text{Mo}(p,2n)^{99\text{m}}\text{Tc}$ differ from the data of ref. [5,6] by a factor of two.

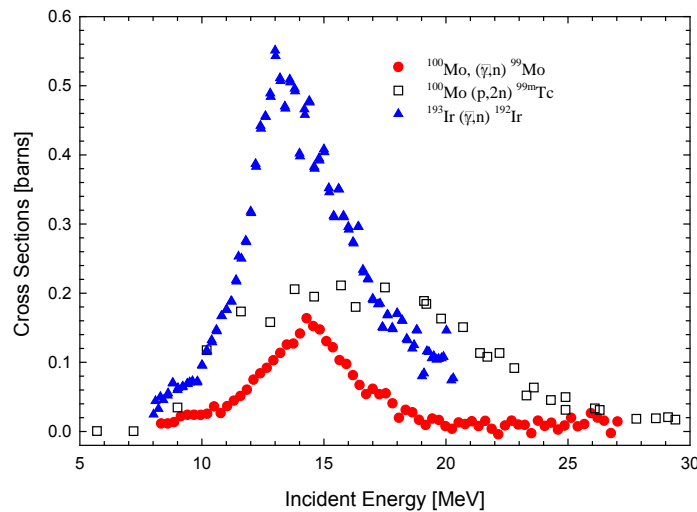


Figure 3. The cross sections for $^{100}\text{Mo}(\gamma, n)$ [7], (p,2n) [5,6] and $^{193}\text{Ir}(\gamma, n)$ [8] reactions versus incident beam energy. Data are taken from <http://www.nndc.bnl.gov>

The GDR centroid for ^{193}Ir (13.3 MeV), calculated from the theoretical expression: $77 \cdot A^{1/3}$, theoretical model described in Reference [4] and illustrated above in Figure 2, is in agreement with that shown in Figure 3 and the width of 3.98 MeV is comparable. However, the corresponding theoretical value for ^{100}Mo is about 2 MeV larger (16.6

MeV) than measured value [7] (see Figure 3), but the width of 5 MeV is comparable. However, the note worthy feature is a maximum cross section at around 14 MeV with a width (FWHM) of about 5 MeV. Thus, one should expect high probabilities for the respective (γ, n) photo-neutron reactions to occur and both photonuclear reactions could be used in production of the respective medical isotopes.

Some examples of calculations will also be mentioned here to compare production of ^{99m}Tc isotope by proton beam with the application of gamma ray beam for ^{99}Mo production. The production of Iridium-192 is of special interest because of the presence of 37% of Iridium-191 in the natural Iridium isotope, therefore the usage of neutrons produced in GDR in additional neutron capture reaction ($^{191}\text{Ir} (n, \gamma) \rightarrow ^{192}\text{Ir}$) is investigated. A well known technique in nuclear reactor technology to employ beryllium foils to serve as reflectors to capture neutrons in the target volume needs to be explored.

2.1 Induced Radioactivity

A process, which produces the radioactive atoms ($N(t)$ at time t) of characteristic mean-life τ can be described by the following equation:

$$N(t \leq t_i) = R\tau(1 - e^{-t/\tau}) \tag{1}$$

$$\left| \frac{dN(t > t_i)}{dt} \right| = R(1 - e^{-t_i/\tau})e^{-(t-t_i)/\tau}$$

where R is the rate of production of the isotope of mean life τ . The rate is a product of the production cross section as the nuclear physics parameter and the experimental conditions of incident beam flux and number of target nuclei. The equilibrium state is reached at times (t) greater than 3τ as shown in Figure 4 (solid line) and it stays almost unchanged. When the irradiation stops, the decay will occur with the characteristic mean life time τ . In Figure 4, the examples are shown where irradiation is assumed to have stopped at $t = 1\tau$ and 3τ . Subsequently, the radioactivity decreases as illustrated in Figure 4.

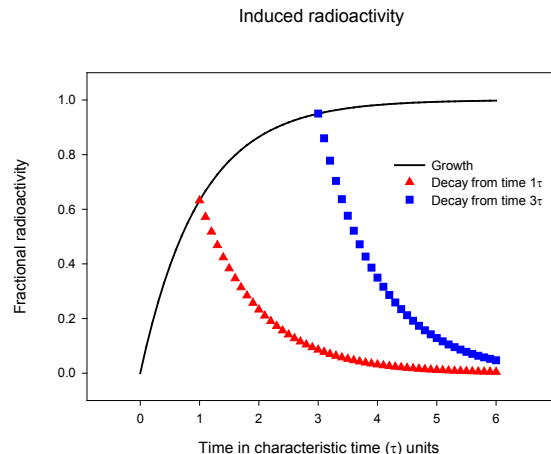


Figure 4. The induced radioactivity and subsequent decays from the time $t = 1\tau$ and 3τ .

The graph above shows that the radioactivity level reaches 95% of the maximum (equilibrium) activity after an irradiation time corresponding to three mean-lives of the product and therefore it is not efficient to irradiate samples for times longer than three mean-lives times of the produced medical isotope. At any time, the number of radioactive atoms does not exceed the value $R\tau$ and thus the activity of the target does not exceed this equilibrium number of the produced radioactive atoms limit.

Photons of energies to carry out the feasibility studies of these reactions are already available at the quasi-monochromatic Laser-Compton gamma-rays produced by Advanced Industrial Science and Technology (AIST) using the electron storage ring TERAS [9] in Japan and also at the HIGS facility of Duke University in USA). The broad resonances (5-3 MeV) as shown in Figures 2 and 3 mean that the experiment should not be very sensitive to either energy spread or the energy calibration of the incoming beam. It is the intent of this paper to suggest that the Canadian Light Source can also play a very important role in this research.

Below, we present the preliminary results of simulations carried out for the isotopes mentioned above. In the present simulation it is assumed that the beam is flat and annular with the 4 mm diameter and the energy spread of the quarter value of the total width of resonance.

3. FLUKA, Monte Carlo, simulation of photo-neutron and proton-neutron reaction transmutation

FLUKA (FLUktuierende KAskade) is a fully integrated Monte Carlo simulation package for the interaction and transport of particles and nuclei in matter [10,11]. It is a general purpose tool for calculations of particle transport and interactions with matter, covering an extended range of applications spanning from proton and electron accelerator shielding to target design, calorimetry, activation, dosimetry, detector design, accelerator driven systems, cosmic ray physics, neutrino physics, radiotherapy etc.

These are preliminary simulations of a toy experiment of transmutation of ^{193}Ir and ^{100}Mo targets induced by photon or proton beam. To get a better statistic one million primaries (photon or proton particles) are used and five to eight runs are performed to estimate error of calculations. The results are calculated per pulse, which is assumed to contain 7×10^{12} particles, or per particle as indicated.

3.1 Isotopes produced in ^{100}Mo target in proton-nuclear and the photo-nuclear reaction

In the present simulation it is assumed that the beam is flat and annular with the 0.004 m diameter. The incident energy is 18 MeV and 14.8 MeV for proton and photon beam, respectively. The energy spread of the quarter value of the total width of GDR resonance

(2.5 MeV) is assumed for both beams. The simulations are performed for target (^{100}Mo) of cylindrical shape with 0.01 m diameter and 0.04 m height. The ^{100}Mo sample is immersed in the spherical lead container (0.3 m radius). In Tables 1 and 2 the number of isotopes produced per one proton and photon particle in one cm^3 ^{100}Mo are shown respectively. The code does not list however the reaction and only yield and error in % is listed in the output of the code.

Table 1

Isotopes produced (per one cm^3 ^{100}Mo target of cylindrical shape with 0.01 m diameter and 0.04 m height, per one proton) in the proton-nuclear reaction. The first column shows the reaction yielding the product nucleus.

Produced Isotope (reaction)	Yield [per one proton/ cm^3]	Error [%]
(p,n) ^{100}Tc	4.84×10^{-04}	2
(p,2n) ^{99}Tc	2.83×10^{-03} (~1.35×10^{-03} ^{99m}Tc)	1
(p,3n) ^{98}Tc	7.60×10^{-06}	13.5
(n, γ) $^{101}\text{Mo}^\#$	2.00×10^{-07}	99
(p,p) ^{100}Mo	9.58×10^{-05}	6.2

$^\#$ Secondary neutron capture.

Table 2

Isotopes produced (per one cm^3 ^{100}Mo target of cylindrical shape with 0.01 m diameter and 0.04 m height, per one photon) in the photo-nuclear reaction. As in Table 1 the first column shows the reaction responsible for the produced nucleus.

Produced Isotope (reaction)	Yield [per one photon/ cm^3]	Error [%]
(n, γ) $^{101}\text{Mo}^\#$	3.40×10^{-06}	15
($\gamma, e^+ e^-$) _{atomic} ^{100}Mo	7.94×10^{-05}	6.8
(γ, n) ^{99}Mo	1.37×10^{-02}	0.3
($\gamma, 2n$) ^{98}Mo	6.32×10^{-03}	0.5

$^\#$ Secondary neutron capture.

Tables 1 and 2 show that both proton and photon induced transmutations in ^{100}Mo yield more than an order of magnitude higher production of the isotopes of interest (^{99}Tc , ^{99}Mo , respectively) than the other isotopes shown there. The amount (1.37×10^{-02}) of ^{99}Mo produced per one photon and one cm^3 of ^{100}Mo (γ, n) is larger than the production (1.35×10^{-03}) of ^{99m}Tc by proton beam. Detailed comparisons can be made only after the beam parameters and target geometry are optimized for proton and photon beams, respectively. At this stage, it is not meaningful to make detailed simulations¹.

¹ While the production of ^{99m}Tc is well advanced (with wide (~1 cm diameter) proton beams that have small energy width (< 2%) and thin film target are used) the application of photo-nuclear reaction is in the developmental stage indicating that both the target (small diameter cylinders) and the beam (wide energy width) will have opposite specification parameters.

3.2 Isotopes produced in ^{193}Ir target in the photo-nuclear reaction.

Now, we discuss the preliminary simulations of transmutation of ^{193}Ir by photon beam. The target and beam are general model parameters, not optimized to any particular facility. The energy of the beam is assumed to be equal to the centroid of theoretical GDR (shown in Figure 2 and equal to 13.3 MeV) and the energy spread is assumed to be 1.9 MeV. The simulations are performed for target (^{193}Ir) of cylindrical shape with 0.01 m or 0.004 m diameter and 0.04 m height. The ^{193}Ir sample is immersed in the spherical lead container (0.3 m radius) while natural Iridium samples are immersed in double spherical containers made from beryllium and lead. The simulated production of residual nuclei per one cm^3 ^{193}Ir cylindrical target with 0.01 m diameter, per one photon particle, is shown in Table 3a. Following recommendations of FLUKA code user manual, in Table 3b, the calculations are repeated with artificial shortening of the photon hadronic interaction length by a factor 0.02 in order to improve statistics. In Table 4a and 4b the simulations are repeated for the ^{193}Ir target with the diameter equal to the diameter of the photon beam (0.004 m). In Tables 5-8 productions of residual nuclei per one cm^3 natural Ir target per photon are shown. Additionally in the first column possible nuclear reaction is listed although code does not list it in the output.

All results presented in Tables 3-8 demonstrate that the production of ^{192}Ir is orders of magnitude more than the others. Examples of detail FLUKA simulation are shown in Appendix A for ^{193}Ir target, photo-nuclear reaction.

Table 3a

Isotopes produced (per one cm^3 ^{193}Ir of cylindrical shape with 0.01 m diameter and 0.04 m height, per one photon) in the photo-nuclear reaction. The spherical lead container (0.3 m radius) is used.

Produced Isotope (reaction)	Yield [per one photon/ cm^3]	Error [%]
$(n,\gamma) ^{194}\text{Ir}$	1.36×10^{-4}	3
$(\gamma, e^+e^-)_{\text{atomic}} ^{193}\text{Ir}$	1.28×10^{-3}	0.8
$(\gamma, n) ^{192}\text{Ir}$	2.04×10^{-2}	0.1
$(\gamma, 2n) ^{191}\text{Ir}$	9.00×10^{-4}	0.9

Table 3b

Isotopes produced (per one cm^3 ^{193}Ir of cylindrical shape with 0.01 m diameter and 0.04 m height, per one photon) in the photo-nuclear reaction. The spherical lead container (0.3 m radius) is used. The photon hadronic interaction length is reduced by a factor 0.02 in order to improve statistics.

Produced Isotope (reaction)	Yield [per one photon/ cm^3]	Error [%]
$(n,\gamma) ^{194}\text{Ir}$	1.33×10^{-4}	0.2
$(\gamma, e^+e^-)_{\text{atomic}} ^{193}\text{Ir}$	1.28×10^{-3}	0.1
$(\gamma, n) ^{192}\text{Ir}$	2.04×10^{-2}	0.04
$(\gamma, 2n) ^{191}\text{Ir}$	9.16×10^{-4}	0.1
$(\gamma, p) ^{192}\text{Os}$	1.97×10^{-8}	42

Table 4a

Isotopes produced (per one cm^3 ^{193}Ir of cylindrical shape with 0.004 m diameter and 0.04 m height, per one photon) in the photo-nuclear reaction. The spherical lead container (0.3 m radius).

Produced Isotope (reaction)	Yield [per one photon/ cm^3]	Error [%]
$(n,\gamma) \text{ } ^{194}\text{Ir}$	4.99×10^{-5}	3.9
$(\gamma, e^+ e^-)_{\text{atomic}} \text{ } ^{193}\text{Ir}$	4.76×10^{-4}	2.0
$(\gamma, n) \text{ } ^{192}\text{Ir}$	2.03×10^{-2}	0.3
$(\gamma, 2n) \text{ } ^{191}\text{Ir}$	4.11×10^{-4}	1.6

Table 4b

Isotopes produced (per one cm^3 ^{193}Ir of cylindrical shape with 0.004 m diameter and 0.04 m height, per one photon) in the photo-nuclear reaction. The spherical lead container (0.3 m radius) is used. The photon hadronic interaction length is reduced by a factor 0.02 in order to improve statistics.

Produced Isotope (reaction)	Yield [per one photon/ cm^3]	Error [%]
$(n,\gamma) \text{ } ^{194}\text{Ir}$	4.4×10^{-5}	0.5
$(\gamma, e^+ e^-)_{\text{atomic}} \text{ } ^{193}\text{Ir}$	4.69×10^{-4}	0.1
$(\gamma, n) \text{ } ^{192}\text{Ir}$	2.03×10^{-2}	0.06
$(\gamma, 2n) \text{ } ^{191}\text{Ir}$	4.12×10^{-4}	0.2
$(\gamma, p) \text{ } ^{192}\text{Os}$	1.69×10^{-8}	34.1

3.3 Isotopes produced in natural Ir in the photo-nuclear reaction.

The natural Ir contains 37% of ^{191}Ir and 63% of ^{193}Ir and thus additional reaction with ^{191}Ir isotopes of target, which is listed in the first column of Tables 5-8 is indicated by an asterisk (*).

Table 5

Isotopes produced (per one cm^3 natural Ir, per one photon) in the photo-nuclear reaction. The spherical lead container (0.3 m radius) is used.

Produced Isotope (reaction)	Yield [per one photon/ cm^3]	Error [%]
$(n,\gamma) \text{ } ^{194}\text{Ir}$	1.23×10^{-4}	2.4
$(\gamma, e^+ e^-)_{\text{atomic}} \text{ } ^{193}\text{Ir}$	1.26×10^{-3}	1.6
$(\gamma, n) \text{ or } (n, \gamma)^* \text{ } ^{192}\text{Ir}$	1.28×10^{-2}	0.5
$(\gamma, 2n) \text{ } ^{191}\text{Ir}$	8.58×10^{-4}	2
$(\gamma, 3n) \text{ or } (\gamma, n)^* \text{ } ^{190}\text{Ir}$	7.6×10^{-3}	0.3

Table 6

Isotopes produced (per one cm³ natural Ir, per one photon) in the photo-nuclear reaction. The spherical beryllium container (0.1m radius) immersed in the lead container (0.4 m radius) is used.

Produced Isotope (reaction)	Yield [per one photon/cm ³]	Error [%]
(n,γ) ¹⁹⁴ Ir	3.19x10 ⁻⁴	1.9
(γ,e ⁺ e ⁻) _{atomic} ¹⁹³ Ir	1.29x10 ⁻³	0.9
(γ,n) or (n,γ)* ¹⁹²Ir	1.31x10⁻²	0.4
(γ,2n) ¹⁹¹ Ir	9.06x10 ⁻⁴	1.7
(γ,3n) or (γ,n)* ¹⁹⁰ Ir	7.51x10 ⁻³	0.3
(γ,p)* ¹⁹⁰ Os	2.0x10 ⁻⁷	99

Table 7

Isotopes produced (per one cm³ natural Ir, per one photon) in the photo-nuclear reaction. The spherical beryllium container (0.2 m radius) immersed in the lead container (0.4 m radius) is used.

Produced Isotope (reaction)	Yield [per one photon/cm ³]	Error [%]
(n,γ) ¹⁹⁴ Ir	3.44x10 ⁻⁴	1.2
(γ,e ⁺ e ⁻) _{atomic} ¹⁹³ Ir	1.29x10 ⁻³	1
(γ,n) or (n,γ)* ¹⁹²Ir	1.32x10⁻²	0.3
(γ,2n) ¹⁹¹ Ir	8.87x10 ⁻⁴	0.4
(γ,3n) or (γ,n)* ¹⁹⁰ Ir	7.56x10 ⁻³	0.9

Table 8

Isotopes produced (per one cm³ natural Ir, per one photon) in the photo-nuclear reaction. The spherical beryllium container (0.3 m radius) immersed in the lead container (0.4 m radius) is used.

(Reaction) Produced Isotope	Yield [per one photon/cm ³]	Error [%]
(n,γ) ¹⁹⁴ Ir	3.52x10 ⁻⁴	1.7
(γ,e ⁺ e ⁻) _{atomic} ¹⁹³ Ir	1.29x10 ⁻³	0.7
(γ,n) or (n,γ)* ¹⁹²Ir	1.33x10⁻²	0.2
(γ,2n) ¹⁹¹ Ir	8.92x10 ⁻⁴	1.1
(γ,3n) or (γ,n)* ¹⁹⁰ Ir	7.55x10 ⁻³	0.3

Table 6-8 indicate that the presence of beryllium enhance production of ¹⁹²Ir isotope only by few percent and the recorded number of residuals of ¹⁹²Ir in lead container for natural iridium are equal to that calculated for pure ¹⁹³Ir multiplied by the fraction of ¹⁹³Ir present in nature (2.04x10⁻² x 0.63 = 1.29 x 10⁻²).

In Appendix A, Figures 5a,b show the geometry of Ir target (of cylindrical shape with 0.01m diameter and 0.04 m height) embedded in the spherical lead container (0.3 m radius). Figures 6a,b show the results of the calculations by FLUKA: (a) dose in pGy per

pulse and (b) equivalent dose in pSv/pulse in lead container and ^{193}Ir sample are shown respectively. One can see that substantial radiation dose (a) is deposited to the target and a few neutrons escape through lead container (b). In Figures 7a,b and 8a,b the photon and neutron fluence per pulse (7×10^{12} photons) produced in ^{193}Ir (γ, n) target (of cylindrical shape 0.01 and 0.004 m diameter, 0.04 m height) in the spherical lead container (0.3 m radius) calculations are shown. In attempt to improve statistics, as suggested by FLUKA, the simulations are repeated by reducing the the photon hadronic interaction length by a factor 0.02. These results are shown in figures labeled 'b'. One can notice improvement in statics for the lower energy neutrons but this improvement does not influence much the number of calculated residuals of ^{192}Ir as shown in Tables 3a,b and 4a,b above. The enhancement of the number of events allows for creation of some protons by (γ, p) reaction. The Figures 9a,b show the plots of the proton and neutron fluence calculated per pulse (7×10^{12} photons) in ^{193}Ir , (γ, n) target (of cylindrical shape (a) 0.01 m and (b) 0.004 m diameter and 0.04 m height) in the spherical lead container (0.3 m radius). Figures 6-9 show evidence that a wide energy range spectrum of neutrons was created during simulations, but the energies for most neutrons are in the region where cross section is too small to produce significant amount of ^{192}Ir isotope. This result should be verified experimentally as for a large range of neutron energy, cross sections are not available and the simulated results rely on extrapolation. To enhance (n, γ) reaction additional layer of moderator is required but it would complicate design of experiment, therefore at the moment it is rather recommended to use pure ^{193}Ir target.

4. Laser Back Scatter Photon Beams

The laser back scatter facilities are now well established as work-horses in Japan and USA. The principle is based on well known Compton scattering of photons by electrons. Unlike the undergraduate experiments where the photons bounce off an electron at rest in the laboratory, the laser back scatter facilities use the relativistic electrons from the beam facilities as the scattering partners. The energy of scattered photons can be written as:

$$E_{\gamma} = \frac{4\gamma^2 E_L}{1 + 4\gamma E_L / m_e c^2 + (\gamma\theta)^2} \quad (2)$$

where $\gamma = E_e / m_e c^2$ is the Lorentz factor of electron beam, $E_L =$ energy of laser photon = $1240 / \lambda$ eV, with λ expressed in nanometers.

The scattering angle θ is zero along the electron beam path. With these definitions, it is seen that for the CLS with $\gamma = 5675$, an industrial CO_2 laser emits photons of 10.6 microns ($E_L = 0.117$ eV) produces photon beams of energies $E_{\gamma} = 15$ MeV at zero degrees. The same laser also emits photons of 9.6 microns, yielding scattered photons of 16.5 MeV energies. Either one of them or the two in combination will serve our purposes.

5. Conclusion

The idea of using MeV photon beams by taking advantage of an ubiquitous feature of nuclear excitations, known as Giant Dipole Resonance (GDR) is explored. The Monte Carlo simulations using the FLUKA for $^{193}\text{Ir}(\gamma, n)$ and natural Ir target show that the production of the $^{192}\text{Ir}(\gamma, n)$ medical and industrial application isotope is of the orders of magnitude higher than the other isotopes, making this technique very promising. The production of ^{99}Mo by photoneutron reaction on ^{100}Mo target is also explored. Detailed comparison to production with proton beams must await specifications of realistic models of experimental arrangements. It is pointed out that the CLS facility equipped with a CO_2 laser back scatter system will serve as a good testing ground to establish the feasibility of this technique.

6. Acknowledgement

Comments and discussions with Katherine Gagnon from the University of Alberta and Prof. Hiro Ejiri, RCNP from Osaka University are acknowledged.

7. References

- [1] The Canadian Neutron Source, proposal by the Government of Saskatchewan and University of Saskatchewan, (July, 2009).
- [2] The Sherbrooke University News Release (January 2010); NSERC, CIHR (Sherbrooke University, TRIUMF, UBC, BC Cancer Agency, University of Alberta, Lawson Health); Executive Summary of the Report of the Expert Panel on Medical Isotopes, "Report on the Expert Panel on Medical Isotopes", CNS Bulletin, vol. 30, No 4 (2009) 17.
- [3] The Prairie Isotope Production Enterprise (PIPE) proposal, (Fall- 2009); TRIUMF Making Medical Isotopes: Report of the Task Force on Alternatives for Medical-Isotope Production (<http://admin.triumf.ca/facility/5yp/comm/Report-vPREPUB.pdf>) (2008).
- [4] S. S. Hanna in Giant Multipole Resonances, topical conferences, Oak Ridge, Tennessee (1979). Ed. Fred Bertrand, Pub: Harwood Academic.
- [5] S. Takacs, Z. Szucs, F. Tarkanyi, A. Hermanne, M. Sonck, "Evaluation of proton induced reactions on ^{100}Mo " J.Rad. Nucl. Chem., 257 (2003) 195.
- [6] B.Scholten, R.M.Lambrecht, M.Cogneau, H.V.Ruiz, S.M.Qaim, "Excitation Functions For the Cyclotron Production of $^{99}\text{M-Tc}$ and ^{99}Mo " Applied Radiation and Isotopes, 51 (1999) 69.
- [7] H. Beil, R. Bergère, P. Carlos, A. Leprêtre, A. De Miniac and A. Veysseyre, "A study of the photoneutron contribution to the giant dipole resonance in doubly even Mo isotopes", Nuclear Physics A227, (1974) 427.
- [8] A.M. Goryachev, Zhurnal. Exper. i Teoret. Fiz., "THE SHAPE OF THE STABLE TRANSITIONAL NUCLEI IR AND PT" 26, (1978) 1479.
- [9] H. Toyokawa a, S.Goko b, S.Hohara c, T.Kaihorid, F.Kaneko, R.Kuroda, N.Oshima, M.Tanaka, M. Koike, A.Kinomura, H.Ogawa, N.Sei, R.Suzuki,

- T.Ohdaira, K.Yamada, H.Ohgaki , “Nuclear Instruments and Methods in Physics Research”, A 608 (2009) S41.
- [10] A. Fasso`, A. Ferrari, J. Ranft, and P.R. Sala, “FLUKA: a multi-particle transport code”, CERN-2005-10 (2005), INFN/TC_05/11, SLAC-R-773.
- [11] G. Battistoni, S. Muraro, P.R. Sala, F. Cerutti, A. Ferrari, S. Roesler, A. Fasso`, J. Ranft, “The FLUKA code: Description and benchmarking”, Proceedings of the Hadronic Shower Simulation Workshop 2006, Fermilab, 6-8 September 2006, M. Albrow, R. Raja eds., AIP Conference Proceeding 896, (2007) 31.

Appendix A

The selected results of FLUKA simulations (photo-nuclear reaction) for the ^{193}Ir target in the lead container (0.3 m radius).

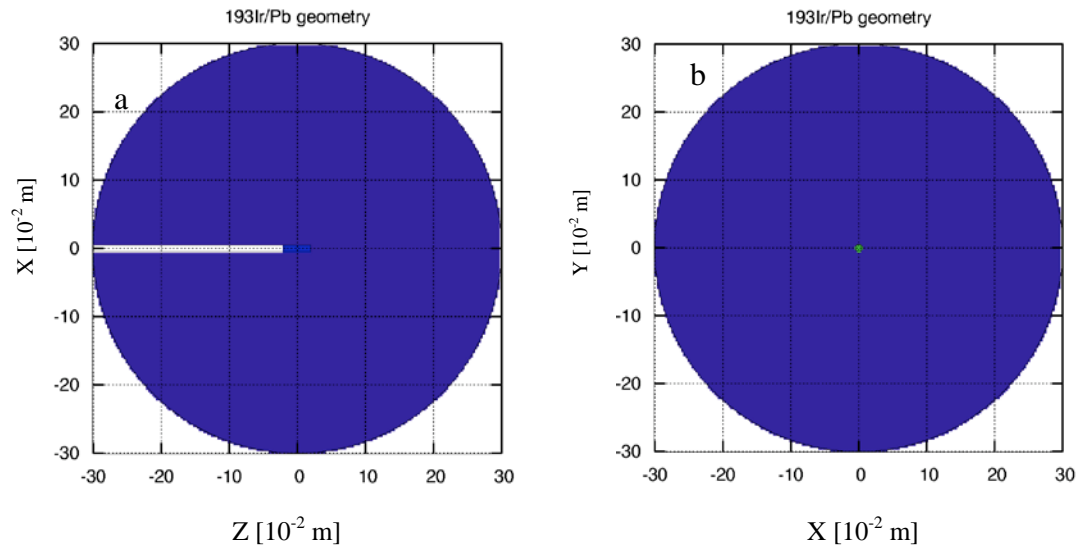


Figure 5a,b. The geometry of Ir target (of cylindrical shape with 0.01m diameter and 0.04 m height) embedded in the spherical lead container (0.3 m radius). It is assumed that the photon beam source is located close to the surface of lead container at the beginning of a shown cylindrical shape channel with the diameter of 0.01m.

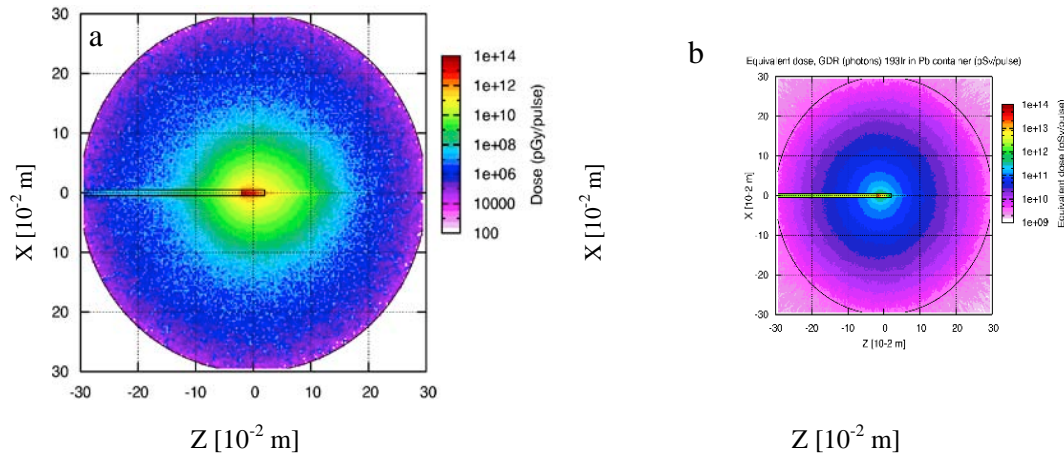


Figure 6a,b. The calculated by FLUKA: a) dose in pGy per pulse and b) equivalent dose pSv/pulse in lead container and ^{193}Ir sample.

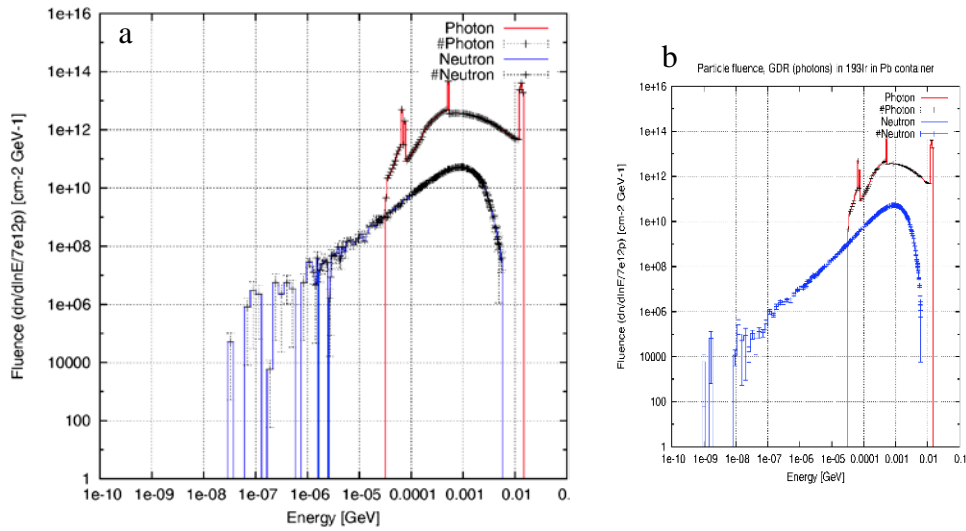


Figure 7a,b. The photon and neutron fluence per pulse (7×10^{12} photons) produced by photo-nuclear reaction in ^{193}Ir target (of cylindrical shape 0.01m diameter and 0.04 m height) in the spherical lead container (0.3 m radius). In (b) the photon hadronic interaction length is reduced by a factor 0.02 in order to improve statistics. The errors are plotted using dotted or solid lines, as indicated.

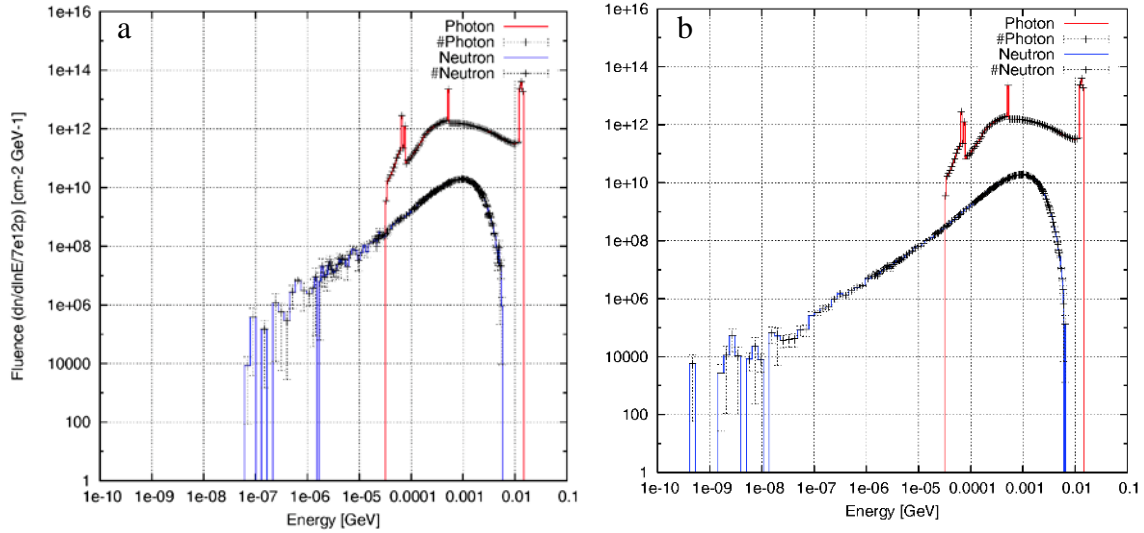


Figure 8a,b. The photon and neutron fluence per pulse (7×10^{12} photons) produced by photo-nuclear reaction in ^{193}Ir target (of cylindrical shape with 0.004 m diameter and 0.04 m height) in the spherical lead container (0.3 m radius). In (b) the photon hadronic interaction length is reduced by a factor 0.02 in order to improve statistics. The errors are plotted using dotted lines, as indicated.

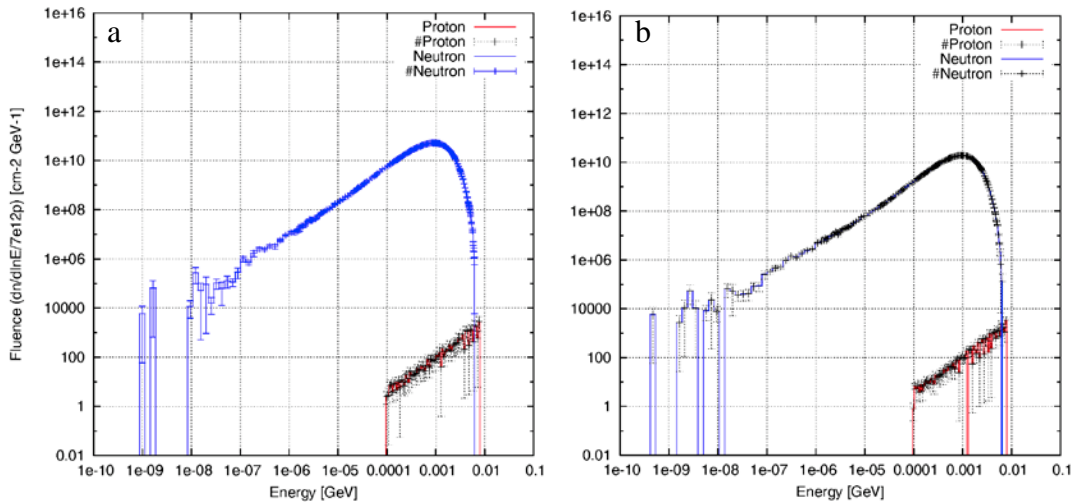


Figure 9a,b. The proton and neutron fluence per pulse (7×10^{12} photons) produced by photo-nuclear reaction in ^{193}Ir target (of cylindrical shape a) 0.01 m and b) 0.004 m diameter and 0.04 m height) in the spherical lead container (0.3 m radius). The photon hadronic interaction length is reduced by a factor 0.02 in order to improve statistics. The errors are plotted using dotted lines, as indicated.